

## Supporting Information

### Preparation of bimetallic nanocrystals by coreduction of mixed metal ions in liquid-solid-solution synthetic system according to the electronegativity of alloys

Junjie Mao, Dingsheng Wang,\* Guofeng Zhao, Wei Jia, Yadong Li  
Department of Chemistry, Tsinghua University, Beijing 100084, P. R. China

\*E-mail: wangdingsheng@mail.tsinghua.edu.cn

#### Experimental Details

*Chemicals:* All the reagents used in this work, including various kinds of metal inorganic salts, NaOH, ethanol, oleic acid, and cyclohexane, were of analytical grade from the Beijing Chemical Factory. They were used without further purification.

*Synthesis:* In a typical synthesis of Pt-Cu nanoparticles, A mixture of 0.5 g of NaOH, 10 ml of oleic acid and 20 ml of ethanol were added into 50 ml of beaker, 0.1 mmol of  $\text{Cu}(\text{NO}_3)_2 \cdot 3\text{H}_2\text{O}$  and 0.15 mmol of  $\text{H}_2\text{PtCl}_6 \cdot 6\text{H}_2\text{O}$  were dissolved in deionized water (5 ml) to form a homogeneous solution, then the solution were added to the above mixture with magnetic stirring for at least 1 hour. The resulting homogeneous solution was transferred to a 40 ml Teflon-lined stainless-steel autoclave. The sealed vessel was then heated at 120 °C for 12 h before it was cooled to room temperature. The resulting products were collected at the bottom of the autoclave, and washed several times with ethanol by centrifugation at 9000 rpm for 8 min.

*Characterization:* The powder XRD patterns were recorded with a Bruker D8-advance X-ray powder diffractometer with  $\text{CuK}\alpha$  radiation ( $\lambda = 1.5406 \text{ \AA}$ ). The size and morphology of as-synthesized samples were determined by using Hitachi model H-800 transmission electron microscope and JEOL-2010F high-resolution transmission electron microscope. Energy dispersive spectroscopy was recorded to determine the composition of the products.

*Catalytic tests:* The Pt-Cu nanocrystals were supported on aluminum oxide by

incipient wetness impregnation method: 3 mg of as-prepared Pt-Cu nanocrystals were dispersed in 10 ml of cyclohexane and 97 mg of aluminum oxide were added into the above solution, which then naturally volatilized under magnetic stirring. The gas-phase selective oxidation of alcohols on these catalysts with molecular oxygen was performed on a fixed-bed quartz tube reactor (700 mm length by 6 mm inner diameter) under atmospheric pressure as described previously.<sup>1</sup> Benzyl alcohol was continuously fed using a high-performance liquid pump in parallel with O<sub>2</sub> (oxidant) and N<sub>2</sub> (diluted gas of 50 ml/min) feeding using calibrated mass flow controllers into the reactor heated to the desired reaction temperature. Weight hourly space velocity (WHSV) was calculated by dividing the mass flow rate of alcohol feedstock by the catalyst mass. The effluent was cooled using an ice-salt bath (-15 °C) to liquefy the condensable vapors for analysis using an Shimadzu-2014 GC gas chromatography-flame ionization detector (GC-FID) with a 60 m HP-5ms capillary column.

1 G. F. Zhao, H. Y. Hu, M. M. Deng, M. Ling and Y. Lu, *ChemCatChem* 2011, **3**, 1629.

### Supplementary Figures

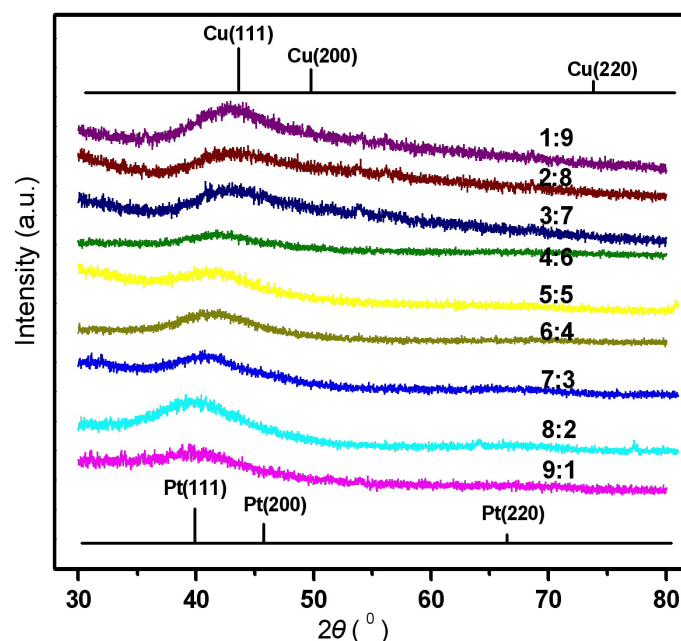


Figure S1. XRD patterns of a series of Pt-Cu nanoparticles.

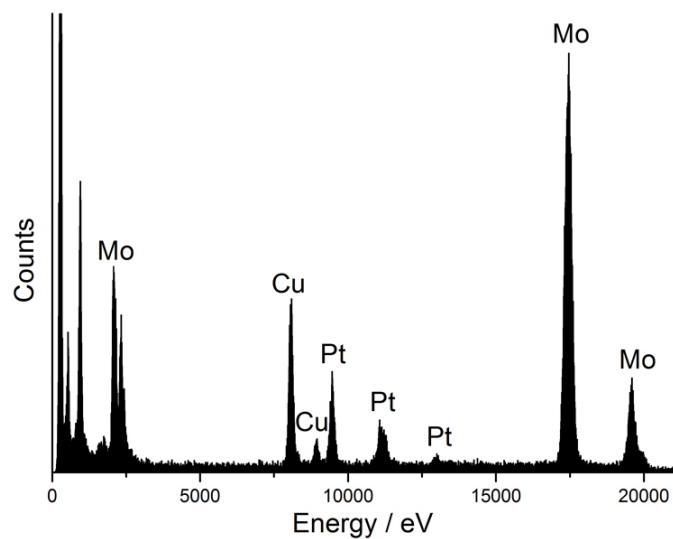


Figure S2. EDS pattern of Pt-Cu nanoparticles.

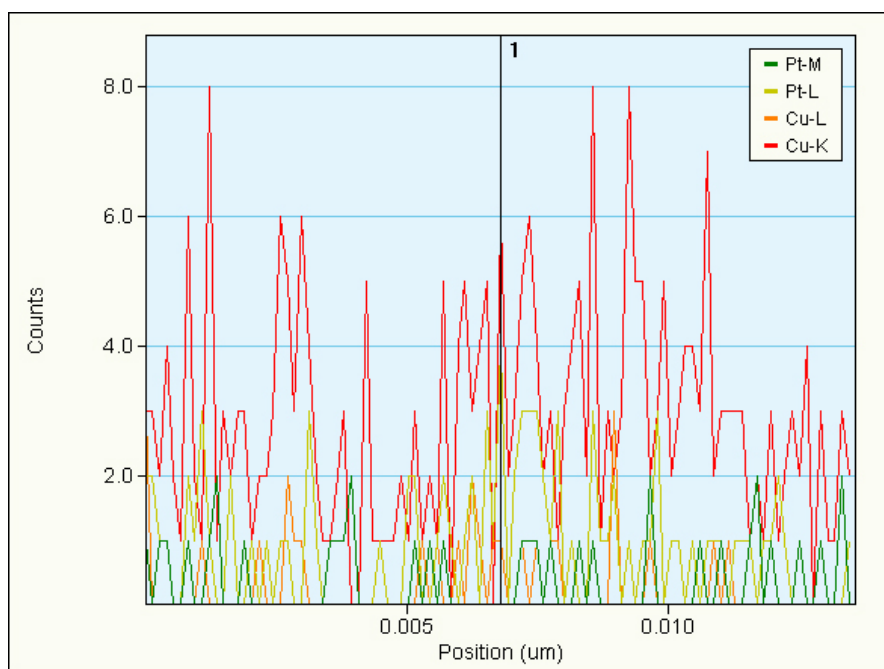


Figure S3. STEM EDS line scanning data of the samples.

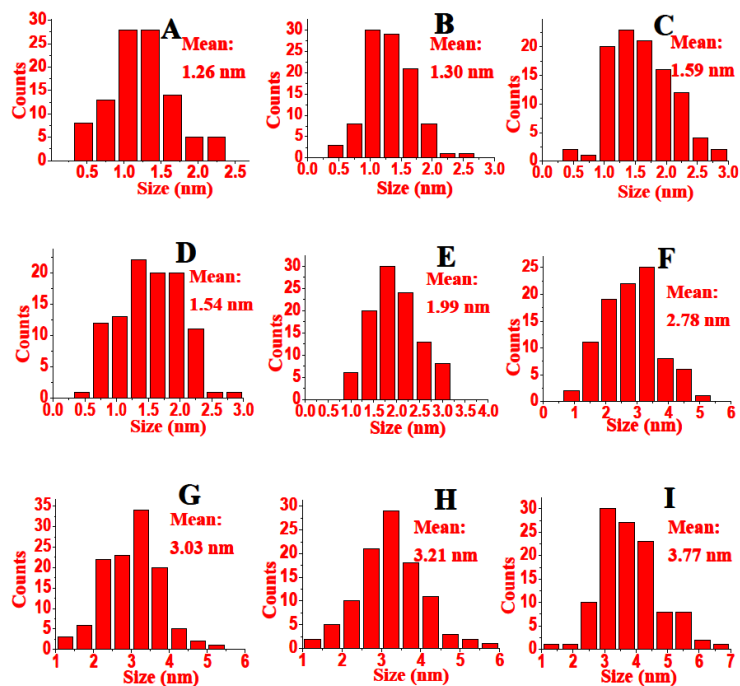


Figure S4. The size distributions of as-obtained A) Pt<sub>0.1</sub>Cu<sub>0.9</sub>, B) Pt<sub>0.2</sub>Cu<sub>0.8</sub>, C) Pt<sub>0.3</sub>Cu<sub>0.7</sub>, D) Pt<sub>0.4</sub>Cu<sub>0.6</sub>, E) Pt<sub>0.5</sub>Cu<sub>0.5</sub>, F) Pd<sub>0.4</sub>Cu<sub>0.6</sub>, G) Pd<sub>0.3</sub>Cu<sub>0.7</sub>, H) Pd<sub>0.2</sub>Cu<sub>0.8</sub>, and I) Pd<sub>0.1</sub>Cu<sub>0.9</sub> nanoparticles.

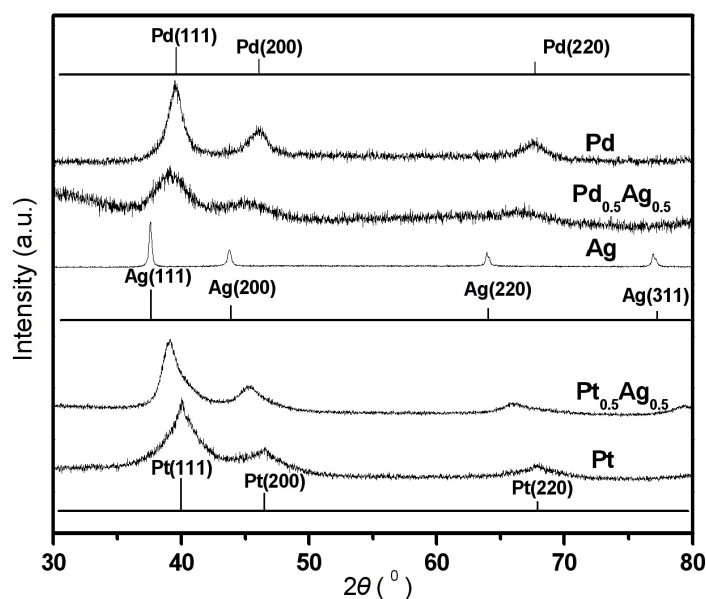


Figure S5. XRD patterns of Pt, Pt<sub>0.5</sub>Ag<sub>0.5</sub>, Ag, Pd<sub>0.5</sub>Ag<sub>0.5</sub>, and Pd nanocrystals.

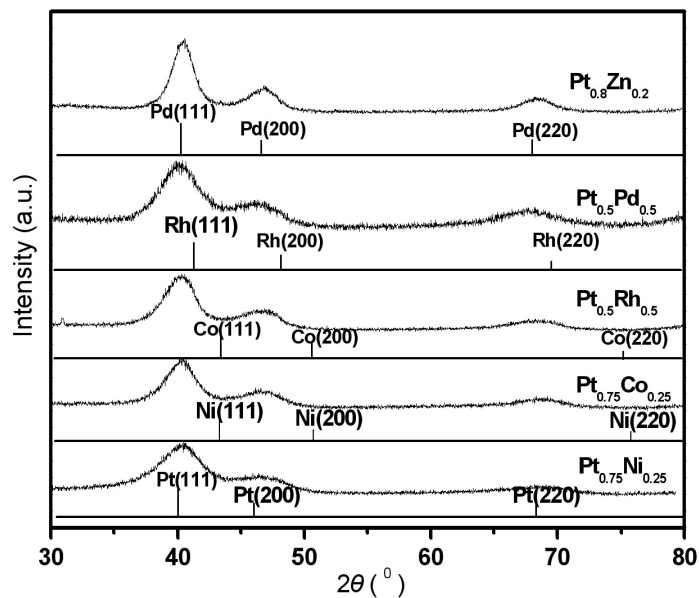


Figure S6. XRD patterns of  $\text{Pt}_{0.75}\text{Ni}_{0.25}$ ,  $\text{Pt}_{0.75}\text{Co}_{0.25}$ ,  $\text{Pt}_{0.5}\text{Rh}_{0.5}$ ,  $\text{Pt}_{0.5}\text{Pd}_{0.5}$ , and  $\text{Pt}_{0.8}\text{Zn}_{0.2}$  nanocrystals.

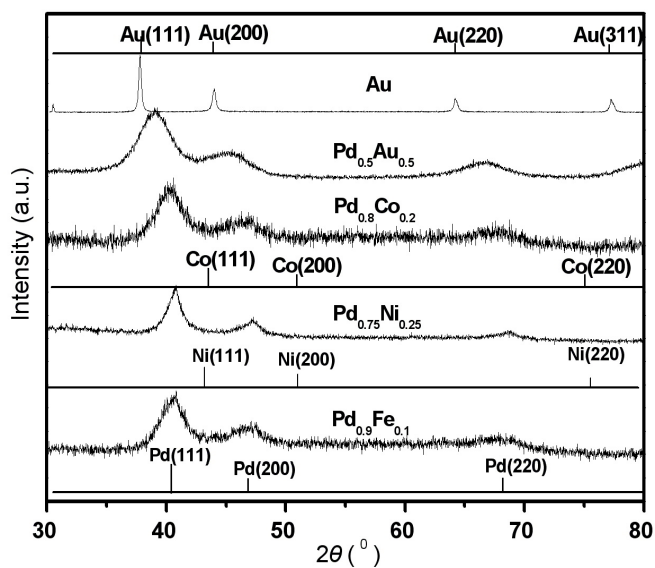


Figure S7. XRD patterns of  $\text{Pd}_{0.9}\text{Fe}_{0.1}$ ,  $\text{Pd}_{0.75}\text{Ni}_{0.25}$ ,  $\text{Pd}_{0.8}\text{Co}_{0.2}$ ,  $\text{Pd}_{0.5}\text{Au}_{0.5}$ , and Au nanocrystals.

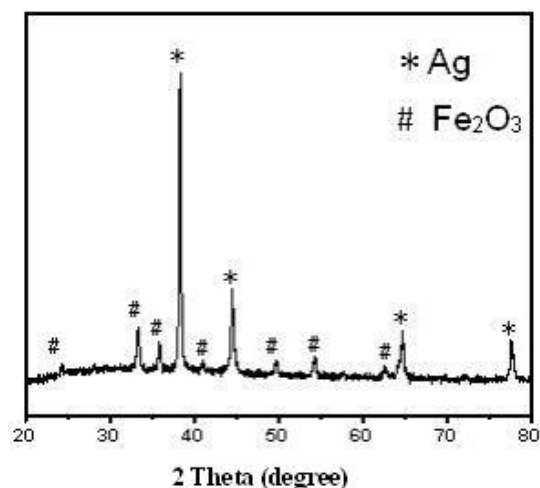


Figure S8. XRD patterns of mixture of Ag and Fe<sub>2</sub>O<sub>3</sub>.

Table S1 The catalytic performance of various catalysts for the gas-phase oxidation of benzyl alcohol.

Catalysts	T <sub>reaction</sub> (°C)	WHSV (h <sup>-1</sup> )	Conversion (%)	Selectivity (%)	Reference
Electrolytic silver	500	8	55	80	1
K/Ag/SiO <sub>2</sub>	300	12	80	99	2
Ag/LTA/Cu-grid	320	50	58	90	3
Ag/Ni-fiber	380	20	86	90	1
Ag/Ni-fiber-M	300	20	90-95	95-99	4
Cu/Na/ZSM-5	400	-	90	90	5
K-Cu-TiO <sub>2</sub>	210	0.6	99	99	8
Au/SiO <sub>2</sub>	315	10	70-80	90-95	6
Au-Cu/SiO <sub>2</sub>	260	10	98	99	7

[1] J. P. Mao, M. M. Deng, Q. S. Xue, L. Chen and Y. Lu, *Catal. Commun.* 2009, **10**, 1376.

[2] R. Yamamoto, Y. Sawayama, H. Shibahara, Y. Ichihashi, S. Nishiyama and S. Tsuruya, *J. Catal.* 2005, **234**, 308.

[3] J. Shen, W. Shan, Y. Zhang, J. Du, H. Xu, K. Fan, W. Shen and Y. Tang, *J. Catal.* 2006, **237**, 94.

[4] M. M. Deng, G. F. Zhao, Q. S. Xue, L. Chen and Y. Lu, *Appl. Catal. B* 2010, **99**, 222.

[5] H. Hayashibara, S. Nishiyama, S. Tsuruya and M. Masai, *J. Catal.* 1995, **153**, 254.

[6] S. Biella and M. Rossi, *Chem. Commun.* 2003, 378.

[7] C. D. Pina, E. Falletta and M. Rossi, *J. Catal.* 2008, **260**, 384.

[8] J. Fan, Y. H. Dai, Y. L. Li, N. F. Zheng, J. F. Guo, X. Q. Yan and G. D. Stucky, *J. Am. Chem. Soc.* 2009, **131**, 15568.